Correlating ground and excited state properties: A quantum chemical study of the photodissociation of the C–N bond in N-substituted anilines

ARTICLE *in* JOURNAL OF MOLECULAR STRUCTURE THEOCHEM · OCTOBER 2002

Impact Factor: 1.37 · DOI: 10.1016/S0166-1280(02)00366-4

3 AUTHORS:

Mikhail Budyka
Russian Academy of Sciences
119 PUBLICATIONS **584** CITATIONS
SEE PROFILE

T. S. Zyubin
Russian Academy of Sciences
63 PUBLICATIONS **404** CITATIONS
SEE PROFILE

Antonios Zarkadis
University of Ioannina
44 PUBLICATIONS **436** CITATIONS
SEE PROFILE

ELSEVIER

Journal of Molecular Structure (Theochem) 594 (2002) 113–125

THEO CHEM

www.elsevier.com/locate/theochem

Correlating ground and excited state properties: a quantum chemical study of the photodissociation of the C–N bond in N-substituted anilines

Mikhayl F. Budyka[a,*], Tatyana S. Zyubina[a], Antonios K. Zarkadis[b]

[a]*Institute of Problems of Chemical Physics, Russian Academy of Sciences, 142432 Chernogolovka, Russian Federation*
[b]*Department of Chemistry, University of Ioannina, 451 10 Ioannina, Greece*

Received 14 January 2002; revised 4 June 2002; accepted 21 June 2002

Abstract

Structure and properties of the ground-state (S_0) and lowest excited singlet (S_1) and triplet states (T_1) of N-substituted anilines PhNH–R (R = CH_3, CH_2Ph, $CHPh_2$, CPh_3) were calculated using semiempirical PM3 method. Ab initio (HF, MP2) and DFT (B3LYP) methods for R = CH_3, CH_2Ph, and HF method for R = $CHPh_2$ were used with 6-31G* and 6-31G** basis sets. All methods predict, in agreement with experiment, a pyramidal S_0 state, which flattens on excitation to S_1 and T_1 ones. The bond dissociation energy (BDE) values of the C–N bond were found to decrease upon insertion of phenyl groups at the benzylic carbon atom. PM3 calculations show, in full agreement with experimental data, that the lowest excited states of anilines studied are in fact the 'local' excited states of the anilino chromophore group. PM3 calculations of the minimal energy path for the C–N bond dissociation in the T_1 state predict a useful Evans–Polanyi linear relationship between activation energy E_a (*excited*-state property) and BDE (*ground*-state property). This enables one to estimate important reactivity parameters (activation energy and rate constant) of an excited state based on an easy accessible ground-state property such as the BDE.

Keywords: MNDO-PM3; Ab initio methods; Substituted anilines; Electronically excited state; Photodissociation

1. Introduction

The dissociation of a chemical bond constitutes a central concept in understanding chemical transformations. While considerable progress has been achieved in rationalizing the factors, which govern the readiness of a molecule to undergo bond fission in the *ground*-state [1,2], the elucidation of the role, which is played by substituent effects in *photo*dissociations, being more complex due to the additional involvement of excited states, remains a challenge [3,4].

$$R_1\text{–}R_2 + h\nu \rightarrow R_1^{\cdot} + R_2^{\cdot}$$

At the same time, the importance of photodissociation reactions is demonstrated in many aspects of applied photochemistry and material science, e.g. photopolymerizations [5,6], photodegradation of organic pollutants [7–9], photostability of dyes and sensitizers [10,11], photoimaging [5] and polymeric materials [12]. In all these examples, the photodissociation ability as

* Corresponding author. Tel.: +7-96-517-1903; fax: +7-96-514-3244.
E-mail address: budyka@icp.ac.ru (M.F. Budyka).

0166-1280/02/$ - see front matter
PII: S0166-1280(02)00366-4

a desired or avoidable property is crucial and should be taken into account in designing material properties. In this connection, dissociation of electronically excited molecules has received significant attention by both experimentalists [3,13,14] and theoreticians [4,15–18]. Especially Michl and Bonacic-Koutecky [15] have pointed out the factors which facilitate the photodissociation of a benzylic σ-bond: (i) high local π excitation energy, (ii) weak σ-bond, (iii) the excitation is into the triplet state (or intersystem crossing is efficient), (iv) dissociating σ-bond perpendicular to the local excited system.

In the present study we describe, how we can get a direct estimate about the photodissociation behavior of a compound, based on a common and relatively easy accessible ground-state property, such as the bond dissociation energy (BDE). In other words, how a ground-state property like the BDE, affects and probably controls the outcome of the excited state as far as its homolytic dissociation is concerned.

We decided to study the C2–N1 bond in N-substituted aniline derivatives **1**–**4** (see structures in Fig. 1) because (1) the C–N bond is a central bond in many common polymers, dyes and organic pollutants (herbicides, etc.), (2) the series **1**–**4** reflects a systematic variation (decrease) of, to a good approximation (see below), only one parameter, the C2–N1 bond strength, and (3) we found recently using laser flash photolysis (LFP), EPR Spectroscopy and product analysis, that they undergo effective decomposition under UV irradiation with fission of this bond [14,19]. Worth-while to note here is also, that the C2–N1 photodissociation proceeds mainly in the triplet excited state [19,20], the quantum yield increases with decreasing BDE [19,20], and all derivatives possess absorption bands in the regions

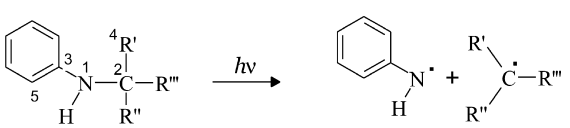

	R'	R"	R'''
1	H	H	H
2	Ph	H	H
3	Ph	Ph	H
4	Ph	Ph	Ph

Fig. 1. General structure of N-substituted anilines studied and atom numbering used.

of 240 and 290 nm and emission bands at ~330 nm, spectral properties characteristic of the lowest excited states of the anilino chromophore. This justifies one to consider the lowest excited states of the anilino group as the local excited states of the molecules **1**–**4**.

2. Methods

The structures, properties, and photodissociation reaction of N-substituted anilines **1**–**4** were studied by means of the semiempirical quantum chemical method MNDO-PM3 [21] (program package MOPAC 7.0). Structures of compounds in the ground and lowest excited states were calculated with full optimization of geometrical parameters. The two simplest members, *N*-methylaniline **1** and *N*-benzylaniline **2**, were calculated using the Hartree–Fock method with 6-31G* and 6-31G** basis sets, correlation corrections were calculated by Moller–Plesset second order perturbation theory (MP2) and density functional theory method (B3LYP). All ab initio and DFT calculations were carried out using the GAUSSIAN94 program package [22].

The lowest singlet excited (S_1) states were calculated by the PM3 method with C.I. = 6 (400 microstates). Preliminary calculations of the triplet states of the anilines and doublet states of the radicals using unrestricted Hartree–Fock (UHF) method showed contamination by higher spin states; for example, $\langle S^2 \rangle$ was 2.23 for the T_1 state of **2**, and 1.21 for the radicals anilino (PhNH) and benzyl ($PhCH_2$) formed through dissociation. Therefore, in further calculations we used the restricted open-shell HF (ROHF) method.

3. Results and discussion

3.1. Geometry

In the ground state for all compounds studied the amino group is calculated to be pyramidal. The degree of nonplanarity (or pyramidality) is conveniently quantified by the sum of the valence angles around the nitrogen atom (ζ values in Table 1). A value of 360° indicates that the nitrogen atom and the three substituents bound to it are coplanar, while $\zeta = 328.4°$

Table 1
Selected geometrical parameters for N-substituted anilines **1**–**4** in the ground (S_0) and lowest excited singlet (S_1) and triplet (T_1) states, optimized by different quantum chemical methods (bond lengths in angstroms, angles in degrees)

Amine	State	r_{C2N1}	r_{C3N1}	∠C3N1C2	ζ^a	Methods
PhNH–CH_3 (**1**)	S_0	1.47	1.44	116.9	339.1	PM3
		1.44	1.39	121.1	347.4	HF/6-31G*
		1.44	1.39	121.2	348.0	HF/6-31G**
		1.45	1.40	119.2	343.7	MP2/6-31G*
		1.45	1.39	121.5	349.4	B3LYP/6-31G*
	S_1	1.47	1.38	119.7	351.3	PM3
	T_1	1.47	1.38	121.1	350.8	PM3
		1.45	1.37	123.4	355.0	B3LYP/6-31G*
PhNH–CH_2Ph (**2**)	S_0	1.48	1.44	117.9	340.3	PM3
		1.45	1.39	121.0	346.5	HF/6-31G*
		1.45	1.39	121.2	347.1	HF/6-31G**
		1.46	1.40	121.6	348.4	B3LYP/6-31G*
	S_1	1.47	1.41	122.2	354.2	PM3
	T_1	1.47	1.39	120.8	349.3	PM3
		1.46	1.37	126.1	356.4	B3LYP/6-31G*
PhNH–$CHPh_2$ (**3**)	S_0	1.50	1.44	118.3	341.3	PM3
		1.46	1.40	121.7	346.7	HF/6-31G*
	S_1	1.48	1.39	123.8	347.8	PM3
	T_1	1.48	1.39	122.3	357.7	PM3
PhNH–CPh_3 (**4**)	S_0	1.52	1.44	122.1	341.8	PM3
	S_1	1.50	1.39	130.1	359.7	PM3
	T_1	1.50	1.38	129.8	359.9	PM3

[a] Sum of the valence angles around the nitrogen atom.

corresponds to a standard tetrahedral geometry. From the microwave data, the sum of the angles in aniline is $\zeta = 345.0°$ [23]. For the substituted anilines studied, the PM3 calculations overestimate pyramidality and predict values of ζ smaller by 3–8° compared to the experimental value of the aniline itself, as well as to the result of more exact calculations (Table 1).

The nitrogen atom is displaced from the plane of the aromatic ring, and the other two substituents are displaced to the opposite side of the ring. For example, in compound **2** (Fig. 2) the N1–C3(aryl) bond deviates from the plane by 5.6° (PM3), corresponding to a deviation of the nitrogen atom by 0.14 Å out of the plane of aniline ring. This is in accordance with the earlier calculations and experimental data for aniline [23–25]. B3LYP gives for **2** a smaller angle 1.8°.

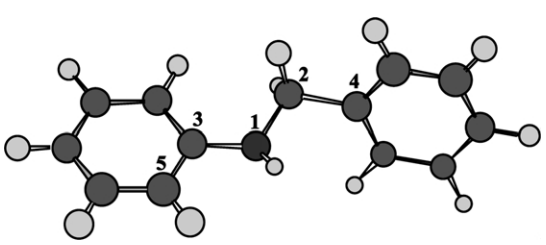

Fig. 2. B3LYP optimized geometry of PhNH–CH_2Ph, **2**.

From Table 1 one can see that every additional phenyl group elongates the C2–N1 bond by 0.01–0.02 Å, and thus the C2–N1 bond is changed from 1.47 to 1.52 Å in the series **1**–**4**. The elongation of the C2–N1 bond is accompanied by a gradual increase in the C3N1C2 valence angle from 117 to 122°. These changes are obviously related to the steric hindrance arising upon insertion of phenyl groups. At the same time the C3–N1 bond remains in all compounds practically unchanged. The two trends found by PM3, elongation of the C2–N1 bond and constancy of the C3–N1 bond length upon progressive phenylation at the aliphatic carbon atom C2, remain in going to the more exact ab initio calculations. However, compared to

PM3, ab initio and DFT calculations result in reduced bond lengths by 0.02 Å for C2–N1 bond and by 0.04 Å for C3–N1 bond (Table 1).

The calculated geometry of the trityl derivative **4** can be compared to the known structure of 5-tritylamino-1,4-dihydronaphthalene, which has the same local arrangement around the C2–N1 bond. According to X-ray data [26], last compound possesses the following bond lengths: Ph_3C–N 1.49 Å; N–C(aryl) 1.40 Å; and C–Ph (three bonds) 1.55, 1.55, 1.53 Å, and valence angles: CNC 125°; NCC(Ph) (three angles) within 106–111°. These experimental values are close to the calculated data for **4** whose bonds lengths are Ph_3C–N 1.52; N–C(aryl) 1.44, and C–Ph (three bonds) 1.54, 1.53, 1.53 Å, and valence angles CNC 122°; NCC(Ph) (three angles) 104–113°.

Fig. 2 shows the geometry of **2** optimized at the B3LYP/6-31G* level. Two phenyl substituents at the C2–N1 bond are in transoid position, ∠C3N1C2C4 = 178.4°, and the C2–N1 bond lies close to the aniline ring plane, ∠C2N1C3C5 = −165.1°.

As was already mentioned in the introduction, one of the factors, which facilitate the dissociation of a benzylic σ-bond, is its perpendicular arrangement in respect to the local excited π-chromophore [15]. However, the B3LYP-optimized structure of **2** shows a deviation from this optimal (perpendicular) arrangement of the C2–N1 bond by 75°. The PM3 method predicts for both the S_0 and T_1 states a slightly lower deviation of 62°. According to PM3 calculation, the ground state conformation with the C2–N1 bond perpendicular to the plane of aniline ring lies ca. 3 kcal/mol over the global minimum.

PM3 predicts that in the lowest singlet excited (S_1) state the aniline system becomes planar (Table 1) and contracts along the long in-plane axis getting a quinoid-like resonance structure; this is in agreement with experimental data and earlier calculations [27–29].

In the lowest excited triplet state (T_1) the main geometry changes compared to the ground-state concerns also the aniline chromophore group; the C3N1 bond decreases by 0.02–0.06 Å, while the valence angle C2N1C3 increases by 3–7° and the nitrogen atom adopts a more planar (compared to S_0) configuration: in some cases the sum of valence angles ζ reaches even 360° (compound **4**, Table 1). Different methods predict slightly different structure for the aniline aromatic ring of the T_1 state. According to PM3, bond lengths between *ipso*- and *ortho*-carbon atoms increase by 0.06 Å, and between *meta*- and *para*-carbon atoms by 0.04 Å, while between *ortho*- and *meta*-carbon atoms decrease by 0.04 Å, i.e. the benzene ring accepts a *para*-quinoid structure. On the contrary, B3LYP predicts antiquinoid structure for the aniline ring. In contrast the geometry of the other groups (benzylic) are practically unchanged. For example, in **2** the aromatic C–C and C–H bond lengths are changed by less than 0.01 Å, while the C2–N1 bond length remains practically constant.

There are no exact experimental data on the geometry of the triplet excited (T_1) aniline chromophore [30]. The $S_1 \rightarrow T_1$ transition has been assumed to be associated with geometry change from planar to presumably nonplanar configuration [31]; investigations in *p*-xylene matrixes at 1.2 K by ESR and microwave-induced delayed phosphorescence (MIDP) indicate that aniline's T_1 state is distorted with the loss of the in-plane two-fold symmetry axis [32]. The conclusion for a slightly distorted geometry is also supported by investigations of aniline's absorption and luminescence spectra in different organic matrixes at 77 K [33]. However, it has been pointed out that the crystal field of the host matrix can be of decisive importance for the average conformation of the triplet state of the guest aromatic molecule [34].

Distinctive charge redistribution takes place upon consecutive phenylation at the aliphatic carbon atom electron density at C2 decreases gradually, and as a result, charge at this atom (S_0 state) changes from −0.31 e for **1** to +0.15 e for **4** (PM3 calculation).

Excitation is associated with charge redistribution mainly on the aniline chromophore with negligible effect on the other phenyl groups. For example, in **2**, PM3 calculations show that on going from S_0 to T_1 state, the charge transfer from nitrogen to *ipso*-carbon of the aniline aromatic ring (atom C3) is equal to 0.25 e, whereas the overall change on the aromatic part of the benzyl group does not exceed 0.01 e, and that on the CH_2 group is within 0.02 e.

Table 2
PM3-calculated heats of formation ΔH_f (in kcal/mol) of aniline derivatives **1**–**4** and corresponding radicals (experimental data are in parentheses)

Amine	ΔH_f	Radical	ΔH_f
PhNH–CH_3 (**1**)	20.58(20.06) [35]	PhNH	60.69(56.7) [36]
PhNH–CH_2Ph (**2**)	46.45	CH_3	29.76(34.82) [37]
PhNH–$CHPh_2$ (**3**)	77.54	CH_2Ph	52.48(49.5) [38]
PhNH–CPh_3 (**4**)	118.24	$CHPh_2$	74.32(66.4) [39]
		CPh_3	101.08(84.5) [38]

3.2. Energy

Heats of formation of the compounds **1**–**4** and the corresponding radicals (PhNH, R) in the ground state are listed in Table 2. Comparison of calculated and known experimental values shows that in some cases the PM3 method underestimates and in other cases overestimates heats of formation of radicals, while at the same time the ΔH_f value for **1** is predicted rather close to the experimental one.

On the basis of the above calculated heats of formation, the BDE values of the C2–N1 bond (Table 3) were evaluated according to Eq. (1):

$$\mathrm{BDE(PhNH{-}R)} = \Delta H_f(\mathrm{PhNH}) + \Delta H_f(\mathrm{R}) - \Delta H_f(\mathrm{PhNH{-}R}) \quad (1)$$

Comparison of calculated BDE for **1** (69.9 kcal/mol) with experimental value (68.9 kcal/mol) [40] shows that in this case the PM3 method predicts BDE rather precisely (within 1 kcal/mol), despite the mistakes in predictions of ΔH_f for radicals PhNH and CH_3 (Table 2). This is explained by the fact that PM3 overestimates ΔH_f for PhNH (by 4 kcal/mol) and underestimates ΔH_f for CH_3 (by 5 kcal/mol), and the two deviations compensate each other. Some discrepancy in the ΔH_f and BDE experimental values of **1** should be noted; calculation of the C2–N1 BDE using ΔH_f experimental data (Table 2) gives a value of 71.46 kcal/mol, that differs by more than 1.5 kcal/mol from the experimental value (68.9 kcal/mol) given in Table 3. Calculation at the HF/6-31* level underestimates BDE for **1** by 10 kcal/mol (ab initio

Table 3
Vertical excitation energies $\Delta(S_{1v} - S_0)$, singlet–triplet energy gaps $\Delta(T_1 - S_0)$, BDEs of the C2–N1 bond in S_0 state, calculated by different methods, and experimental data for **1**–**4** (in kcal/mol)

Amine	$\Delta(S_{1v} - S_0)$	$\Delta(T_1 - S_0)$	BDE	Method
PhNH–CH_3 (**1**)	108.0	51.0	69.9	PM3
			58.4	HF/6-31G*//HF/6-31G*
			58.0	HF/6-31G** //HF/6-31G**
			84.8	MP2/6-31G*//HF/6-31G*
		79.6	73.7	B3LYP/6-31G*//B3LYP/6-31G*
	97.05 [19]		68.9 [39], 71.5[a]	Experimental
PhNH–CH_2Ph (**2**)	107.4	52.3	66.7	PM3
			51.0	HF/6-31G*//HF/6-31G*
			50.8	HF/6-31G** //HF/6-31G**
			77.9	MP2/6-31G*//HF/6-31G*
			78.1	MP2/6-31G** //HF/6-31G**
		85.5	61.0	B3LYP/6-31G*//PM3
		80.7	58.1	B3LYP/6-31G*//B3LYP/6-31G*
	97.3 [19]			Experimental
PhNH–$CHPh_2$ (**3**)	107.9	52.0	57.5	PM3
			45.3	HF/6-31G*//HF/6-31G*
	97.9 [19]			Experimental
PhNH–CPh_3 (**4**)	107.4	51.5	43.5	PM3
	97.9[b] [19]			Experimental

[a] Calculated from experimental data (Table 2), see text.
[b] Shoulder.

and DFT BDE values correspond to the differences of the full energies), whereas electron correlation correction at the MP2/6-31G*//HF/6-31G* level overestimates BDE by 16 kcal/mol compared to experiment (Table 3). B3LYP-calculated BDE value is in good agreement with experimental one. As a whole, it has been shown [41] that DFT method correctly describe the C–N BDE values.

In contrast to **1**, in the case of **2**, the two deviations are summed, since the ΔH_f values for both radicals, PhNH and $PhCH_2$, are overestimated. Therefore, one can expect that PM3 overestimates the BDE for **2** (66.7 kcal/mol, Table 3). Indeed, on the basis of the difference in the BDEs between CH_3–H (105 kcal/mol) and $PhCH_2$–H (88 kcal/mol), and using BDE of the C2–N1 bond in PhNH–CH_3 (68.9 kcal/mol), the value ~52 kcal/mol has been estimated for the C2–N1 BDE in **2**. Comparing BDE values for **1** and **2**, one can see (Table 3), that for these two compounds, variation of about 27 kcal/mol is calculated depending on the methods used: the HF value is the lowest, the MP2 value is the highest, and the B3LYP value is an intermediate and close to the experimental one. The same ratio between BDE values calculated by different methods, HF < B3LYP < MP2, has been reported earlier for the computation of the O–H BDEs in phenols [42].

As follows from PM3 data, the sequential insertion of phenyl groups at the C2 atom in the series **1**, **2**, **3**, **4** results in gradual reduction of the BDE and the trend is comparable to the experimental data of the series CH_3–H (105) [36], $PhCH_2$–H (88) [36], Ph_2CH–H (82) [36], Ph_3C–H (75 kcal/mol) [43]. The phenyl substitution effect on the BDE in the series **1**, **2**, **3** calculated at the HF/6-31G* level decreases from 7.4 (from **1** to **2**) to 5.7 kcal/mol (from **2** to **3**); the effect of the first group, calculated at B3LYP/6-31G* level (from **1** to **2**, 15.6 kcal/mol) is very close to the experimentally observed one in the series of substituted methanes. From comparison with ab initio and DFT data it follows that predicted by PM3 method trend in BDE values is qualitative rather than quantitative.

Substituent effects on BDEs in aromatic systems can ordinary be divided into polar and radical contributions [1,42,44]. As far as the aniline residue in **1**–**4** does not change, the decrease in the BDE on going from **1** to **4** can be attributed entirely to the radical stabilization effect due to delocalization of the unpaired electron. From the above discussion it follows that PM3 underestimates relative stabilization of the methyl radical by introduction of the first phenyl group and overestimates relative stabilization of the diphenylmethyl radical by insertion of the third phenyl group. The C2–N1 bond lengths of **1**–**4** decrease with increasing BDE, in line with the known fact that the two parameters are directly interrelated [45].

The main purpose of the present paper is an attempt to find the way for direct estimation of the photodissociation ability of a compound. For this purpose, calculated BDE values should be compared to excited-state parameters.

Table 3 shows calculated data for the excited states. The heats of formation of compounds in the lowest Franck–Condon excited state (S_{1v}) were calculated using equilibrium geometry of the ground (S_0) state. The difference $\Delta(S_{1v} - S_0)$ corresponds to the maximum of the long-wave absorption band. Data for the lowest triplet excited state T_1 were calculated with complete geometry optimization.

One can see that the PM3 method predicts for all aniline derivatives near the same vertical excitation energies $\Delta(S_{1v} - S_0)$. This is consistent with the experimental data and indicates that the Franck–Condon transition $S_0 \rightarrow S_1$ is localized on the aniline chromophore, being the same in all compounds. Comparison with experimental data shows, that PM3 overestimates the vertical excitation energies by a constant value of ca. 10 kcal/mol. For all aniline derivatives PM3 predicts also near the same energy for all lowest excited triplet state (values of the singlet–triplet gap $\Delta(T_1 - S_0)$ in Table 3). Comparison of the calculated data for **1**–**4** with experimental values for aniline itself in nonpolar solvents (77 [46], 79 kcal/mol [32]) indicates that PM3 underestimates by a constant value the singlet–triplet gap, whereas B3LYP predicts this value rather well.

3.3. Molecular orbitals

Fig. 3 shows the structure of the frontier molecular orbitals (MOs) for **2**: the highest occupied MO (HOMO) and the lowest unoccupied MO (LUMO) of the S_0 state, the lowest semioccupied MO (LSOMO) and the highest semioccupied MO

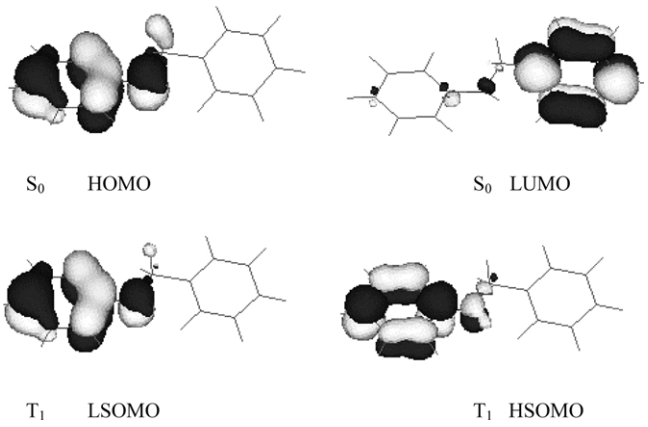

Fig. 3. Structure of the frontier molecular orbitals for *N*-benzylaniline **2**: the HOMO and the LUMO for S_0 state; the lowest semioccupied MO (LSOMO) and the highest semioccupied MO (HSOMO) for T_1 state.

(HSOMO) for T_1 state (the same SOMOs are observed also for the S_1 state).

One can see that in the ground state HOMO is localized on the anilino chromophore with a large contribution by the nitrogen atomic orbital (AO), in contrast LUMO is localized to a large extent to the aromatic part of the benzylic group. It should be noted, that LUMO + 1 is localized on the benzyl group too, while LUMO + 2 and LUMO + 3 at the anilino group. The energies of these four LUMOs are rather close to each other (within 0.4 eV). Next LUMO + 4 lies much higher (by 2 eV) and is antibonding in respect to the C2–N1 bond (σ^* orbital) with some contribution to the aromatic carbon AOs of the benzylic group.

Upon excitation, as a result of relaxation, LUMO + 3 is occupied instead of LUMO. Therefore, in the lowest excited states (S_1, T_1) both SOMOs are localized on the anilino chromophore with large contribution to the AO of the *ipso*-carbon atom C3 (Fig. 3).

The structures of the HOMO in the ground-state and SOMOs in the excited states indicate that the excitation is localized on the anilino group. This has two consequences: first the geometry change of the anilino group in the S_1 and T_1 states, and second the charge redistribution is restricted in electron transfer from nitrogen atom to *ipso*-carbon atom of the aniline ring. This agrees also with the fact that variation of substituents at the benzylic carbon atom has little effect on the excitation energy and positions of the S_1 and T_1 (Table 3).

3.4. The C2–N1 photodissociation reaction

As was already mentioned in Section 1, the photodissociation of *N*-benzylaniline derivatives proceeds mainly in the triplet excited state. However, as was shown in Sections 3.1–3.3, the (equilibrium) lowest triplet (T_1) state of **1**–**4** is in fact the 'local' excited state of the anilino chromophore, which is not dissociative with respect to the C2–N1 bond.

In this connection, the potential energy surface (PES) of the triplet excited state of **2** was investigated in more detail considering the C2–N1 bond length as a reaction coordinate. The calculations were performed keeping the distance of the C2–N1 bond each time fixed, and all other parameters optimized. The obtained curve (minimal energy path) is shown in Fig. 4a. Analysis of the second derivative of the energy shows that the transition state (maximum) on the reaction coordinate at point C ($r_{CN} = 1.97$ Å) is a saddle point (one imaginary frequency).

Before any further discussion on the data, it is worth-while to mention the results of experimental and theoretical investigations of the photochemical properties of methylamine, the simplest compound possessing a C–N bond. Under irradiation at the first ultraviolet absorption band ($\lambda_{max} \sim 215$ nm), methylamine decomposes through several bond fission and molecular elimination channels [47]. One of these channels corresponds to the C–N bond photocleavage.

High-level ab initio quantum chemical calculations

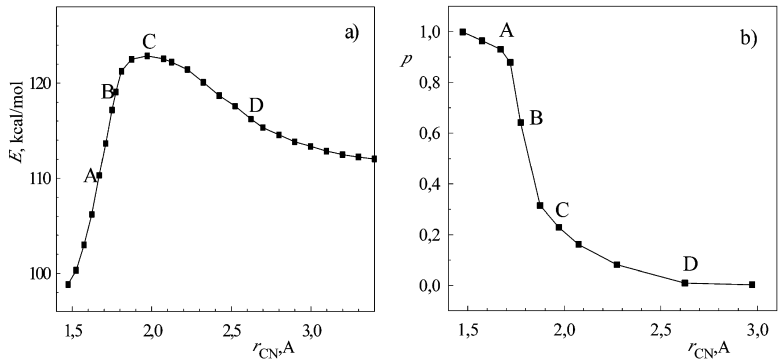

Fig. 4. PM3 calculated data for the dissociation of the *N*-benzylaniline **2** in the lowest excited triplet state (T_1) (structure of molecular orbitals at point A, B, C, and D see in Fig. 5); (a) PES section calculated using the C2–N1 bond length as reaction coordinate (minimal energy path), (b) C2–N1 bond order (p) during elongation of this bond.

show that excitation of methylamine in the first absorption band results in electron transition from nitrogen lone pair to 3s Rydberg orbital. Therefore, in the Franck–Condon region, the lowest excited state is of the *n*, 3s type and not a valence *n*, σ^* one [17,18]. Calculation of the PES of the excited state shows a barrier along the C–N reaction coordinate [17,18]. As the C–N bond is lengthened, the Rydberg s orbital mixes with the σ^*_{C-N} orbital (so called de-Rydbergization), and a transition state results from avoided crossing between two states. On the dissociation limit, the singly occupied orbitals consist of a nitrogen p orbital and a carbon p orbital belonging to the radical fragments NH_2 and CH_3, respectively. These are as well the ground-state dissociation products [18].

Obviously, the photodissociation reaction of **2** can be compared with that of methylamine. These two amines differ, however, by the two phenyl substituents at the nitrogen and carbon atoms, which give rise to differentiation in the spectroscopic minima: unlike methylamine, the lowest excited states of **2** in the Franck–Condon region are π, π^* in nature, possessing partial charge transfer character.

On the other hand, like methylamine, **2** undergoes C2–N1 bond fission upon excitation [19], a fact indicating an interaction between the π^* aniline orbital involved in the excitation and the antibonding σ^*_{C-N} orbital representing the reactive configuration. As the C2–N1 bond is lengthened, these two orbitals mix, and a transition state results from the avoided crossing between the two potential energy surfaces corresponding to the bound spectroscopic (local excited) and reactive (dissociative) configurations. The mixing of these two orbitals of different configurations along the reaction coordinate can be clearly observed upon examination of the MO's structure at the characteristic points A, B, C, D of Fig. 4, see Fig. 5. In the Franck–Condon region (Fig. 5A), both semi-occupied MOs (SOMOs) are localized on the anilino chromophore (see also Fig. 3 and the more detailed discussion in Section 3.3). As the C2–N1 bond is lengthened and the system approaches an energy barrier (Fig. 4, point B), the contribution of the σ^*_{C-N} MO to the HSOMO gradually increases (Fig. 5, point B). In the transition state at the top of the barrier, HSOMO represents mainly the σ^*_{C-N} orbital (Fig. 5, point C), with contribution by the benzylic π-orbital. Beyond the transition state, the singly occupied orbitals are in fact those of the separated anilino (PhNH) and benzyl ($PhCH_2$) radicals, Fig. 5 (point D). This correlates well with the ground state dissociation products.

In line with the above observations are also the changes of the C2–N1 bond order along the reaction pathway (Fig. 4b). When the C2–N1 bond is lengthened, while still remaining near the spectroscopic minimum ($r_{CN} \sim 1.5–1.7$ Å), the bond order decreases only slightly from 1.00 to 0.93. As the system approaches the maximum of the energy barrier and the antibonding σ^*_{C-N} orbital mixes strongly with aniline's π^* MO at $r_{CN} \sim 1.7–2.0$ Å (as was shown above), the C2–N1 bond order falls off rapidly by 0.77. Beyond the transition state ($r_{CN} > 2.0$ Å) the

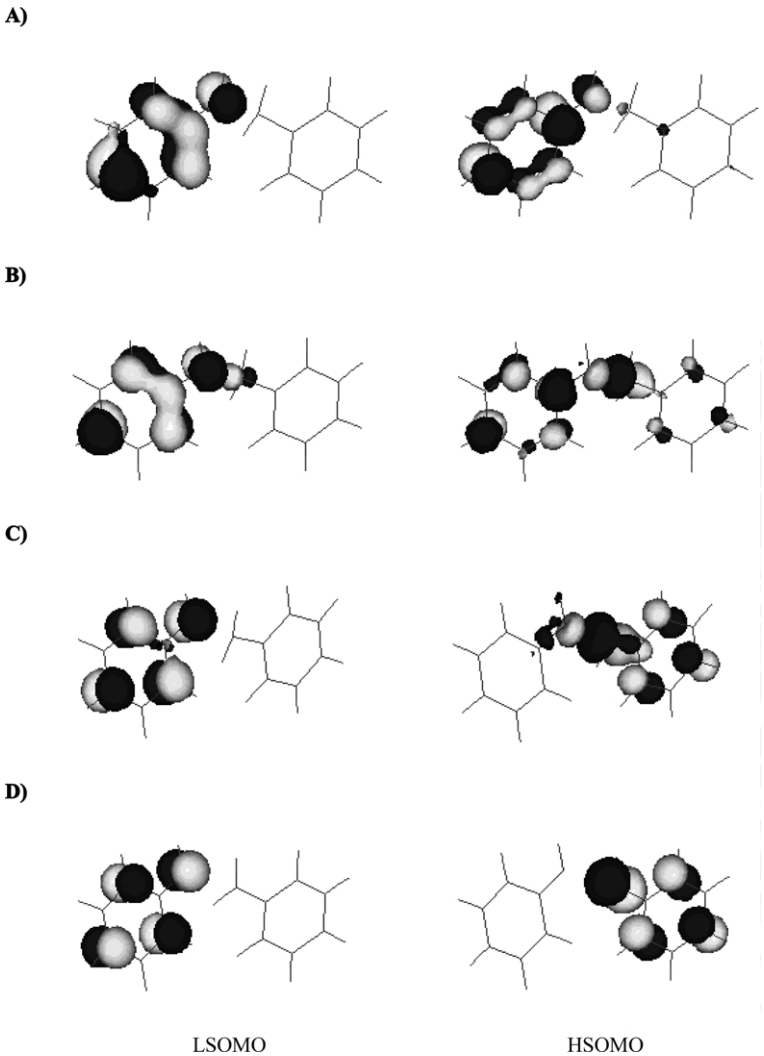

Fig. 5. Structure of the lowest (LSOMO) and highest (HSOMO) semi-occupied MOs at characteristic points A, B, C, and D (Fig. 4) along the reaction coordinate of the dissociation of *N*-benzylaniline **2** in the lowest excited triplet state (T_1): (A) $r_{CN} = 1.67$ Å (at point A); (B) $r_{CN} = 1.77$ Å (at point B); (C) $r_{CN} = 1.97$ Å (at point C); (D) $r_{CN} = 2.62$ Å (at point D).

system consists of practically two separate radicals (PhNH and $PhCH_2$).

The dissociation reaction of the compounds **1**–**4** (PhNH–R), both in S_0 and in T_1, gives rise to the same radical products PhNH and R, see Fig. 6. Therefore, the heat of the C2–N1 bond dissociation reaction (ΔH_r) in the lowest excited triplet state can be calculated similar to the method used for the BDEs:

$$\Delta H_r = \Delta H_f(\text{PhNH}) + \Delta H_f(\text{R}) - \Delta H_f(T_1(\text{PhNH–R})), \quad (2)$$

where $\Delta H_f(T_1(\text{PhNH–R}))$ is the heat of formation of the T_1 state of **1**–**4**. The data obtained, together with calculated activation energies (E_a) and the C2–N1 distances at barrier tops, are listed in Table 4.

We see, that value of ΔH_r reduces with increased phenylation. According to PM3, the dissociation of the first three members (**1**–**3**) of the series is endothermic, but the reaction of the last member (**4**) is exothermic. At the same time, B3LYP predicts an exothermic dissociation already for amines **1** and **2**.

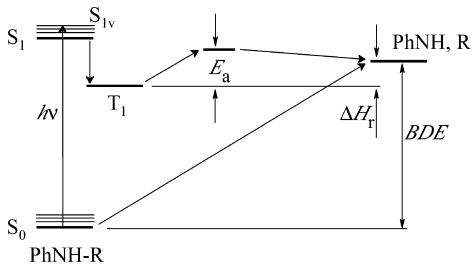

Fig. 6. General energetic scheme considering $\Delta(T_1 - S_0)$, BDE, ΔH_r, and E_a.

As in the case of BDE, the PM3 method correctly predicts the general trend of decreasing ΔH_r with increasing number of phenyl groups, however, the effect of the first group (4.6 kcal/mol) is underestimated and that of the last one (13.5 kcal/mol) is overestimated. In contrast, the effect of the first group, calculated at the B3LYP/6-31G* level is much greater, 16.7 kcal/mol, and is comparable with the effect on BDE. However, these tendencies in BDE and ΔH_r are directly correlated through the linear relationship (3):

$$\Delta H_r = \text{BDE} - \Delta(T_1 - S_0) \quad (3)$$

which derives from the energetic considerations in Fig. 6. From Fig. 6 it is clear that for every specific compound, taken separately, and for every particular dissociating bond, relationship (3) is correct. However, for a homologous series of compounds having the same local chromophore (and therefore, the same local triplet excited state), and the same dissociating bond, the more general conclusion can be made: the heat of the bond dissociation reaction in the lowest excited triplet state is in straight-line dependence on the dissociation energy of this bond. Because amines **1**–**4** are exactly such homologous series of compounds with the same local triplet excited state (average $\Delta(T_1 - S_0)$ value for these amines = 51.7 kcal/mol, see Table 3), Eq. (3) is converted to

$$\Delta H_r = \text{BDE} - 51.7 \text{ (kcal/mol)}. \quad (4)$$

The plot in Fig. 7a shows pictorially this relationship between PM3-calculated values of BDE and ΔH_r for **1**–**4**.

In addition, from Table 4 one can see that the reduction of ΔH_r is accompanied, (i) by the reduction of the activation energy (E_a) and (ii) by the reduction of the C2–N1 distance in the transition state (r_{CN}), indicating an earlier transition state. Last observation agrees with the increased exothermicity down the series **1**–**4**. Quantitatively, the relationship between E_a and ΔH_r (PM3 values) for the dissociation reaction of compounds **1**–**4** in the T_1 state is described by Eq. (5), and graphically depicted in Fig. 7b.

$$E_a = 18.3 + 0.45\Delta H_r \text{(kcal/mol)} \quad (5)$$

This appears to be similar to the Evans–Polyani equation, well known in the ground-state bond dissociation reactions [48]. Through Eqs. (4) and (5) one is allowed to establish a direct quantitative relationship between E_a and BDE, the first being an excited state parameter and the second a ground-state one.

$$E_a = -4.96 + 0.45\text{BDE} \quad (6)$$

This relationship indicates that the activation energy and consequently the rate constant and the quantum yield of the photodissociation of the C2–N1 bond in **1**–**4** can be controlled by a fundamental and easily accessible ground-state property such as the BDE. This enables one to

Table 4
Calculated C2–N1 interatomic distance in the transition state r_{TS} (in Å), activation energy E_a and heat of the C2–N1 bond dissociation reaction ΔH_r (in kcal/mol) in the lowest excited triplet state T_1 for the anilines **1**–**4**

Aniline	r_{TS}	E_a	ΔH_r	Method
PhNH–CH_3 (**1**)	2.12	27.3	18.9	PM3
			−5.9	B3LYP/6-31G*//B3LYP/6-31G*
PhNH–CH_2Ph (**2**)	1.97	24.0	14.3	PM3
			−24.5	B3LYP/6-31G*//PM3
			−22.6	B3LYP/6-31G*//B3LYP/6-31G*
PhNH–$CHPh_2$ (**3**)	1.84	21.1	5.5	PM3
PhNH–CPh_3 (**4**)	1.81	14.6	−8.0	PM3

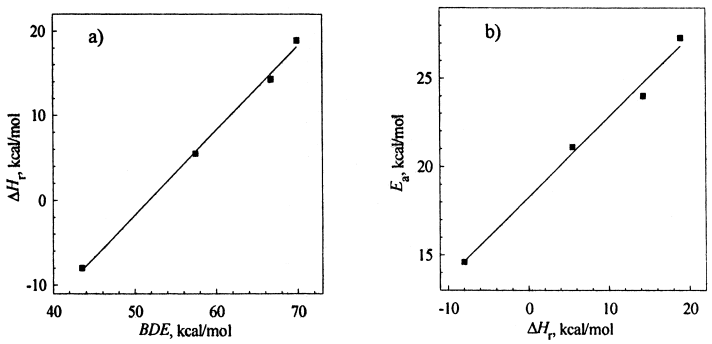

Fig. 7. Correlation between PM3-calculated data for amines **1**–**4**: (a) energy of the C2–N1 bond dissociation ΔH_r in the triplet excited (T_1) state vs. BDE in the ground (S_0) state (correlation coefficient is 0.999); (b) activation energy E_a vs. energy ΔH_r of the C2–N1 bond dissociation reaction in the triplet excited (T_1) state (correlation coefficient is 0.995).

have a quantitative estimate about the ability of a compound to undergo photocleavage. This conclusion is supported experimentally through the measuring of the quantum yields of the photodissociation of **2**, **3**, **4** [14,19,20] and other derivatives, which increase as the C2–N1 bond strength weakens.

It is noteworthy to compare the results obtained here with earlier theoretical considerations. Pearson, discussing a correlation of electronic spectra with chemical reactivity in terms of perturbation theory, has suggested a close relationship between vertical excitation frequency of the lowest excited state and BDE in groups of related molecules [49]. In the aniline derivatives under discussion a correlation between the vertical excitation energies $\Delta(S_{1v} - S_0)$ and BDEs does not exist, see Table 3; this is in line with our findings that the excitation of the first absorption band is localized on the aniline chromophore and does not affect the dissociative σ^*_{CN} orbital. Grimme has investigated the homolytic photodissociation of the C–O bond in aromatic compounds of the type PhO–R by using molecular orbital theory [50], and concluded, that only minor dependence of the reaction efficiency on BDE is expected. He has also suggested that the same should be expected for other carbon-heteroatom photodissociations of compounds of the type PhX–R, where X = O, NR′, S, etc. As we saw, in the case of the aniline derivatives PhNR′–R, this suggestion is not justified, and a straight-line relationship between activation energy E_a of the dissociation in the triplet excited state and BDE is obtained.

4. Conclusions

The photodissociation ability of a material is crucial for many important processes and applications (e.g. photoinitiators, photodegradation of organic pollutants, photochromic materials, sensitizers), and a way of estimating or even of predicting it, based on some relatively easy accessible ground-state property (such as the BDE), would be of invaluable importance.

In the present work, the BDE values for series of N-substituted anilines **1**, **2**, **3**, **4** were calculated using semiempirical PM3 method. Ab initio (HF, MP2) and DFT (B3LYP) methods for **1**, **2**, and HF method for **3** were used with 6-31G* and 6-31G** basis sets. All methods predict the gradual decrease of the C–N BDE values with the sequential insertion of phenyl groups at the benzylic carbon atom.

It was shown that the photofragmentation ability is directly related to the magnitude of the BDE of that bond. Specifically, calculations of the minimal energy paths for the C2–N1 dissociation reaction in the T_1 state predict that the activation energy E_a decreases as the C2–N1 bond becomes weaker down the series of **1**–**4**. Moreover, E_a is connected to the corresponding BDEs through a linear relationship, and consequently the rate constant and the quantum yield of the photocleavage can be directly estimated based on the relatively easy accessible ground-state property BDE. First experimental results [14,19,20] on the photodissociation of **2**–**4** confirm this finding.

Calculations also help to understand the mechanism of the above photodissociation and the derived

relationships. They predict, in full agreement with experimental data, that the lowest excited states of N-substituted anilines **1**–**4** are in fact the 'local' excited states of the anilino chromophore group. The progressive phenylation at the benzylic carbon atom has little effect on the excitation energy, the position of T_1 level, and the geometry and charge distribution within the excited anilino group. Upon dissociation of the C2–N1 bond in the T_1 state, the aniline π^* orbital, which represents the triplet spectroscopic configuration, interacts with the C2–N1 bond σ^* orbital, which represents the reactive configuration. As the C2–N1 bond is lengthened, the two orbitals mix, and a transition state with a certain barrier E_a results from the avoided crossing between the two potential energy surfaces, representing the spectroscopic (local excited) and the reactive (dissociative) configurations. N-substituted anilines **1**–**4** represent thus, a well defined model of the homologous series of compounds having the same 'local' chromophore and different C2–N1 bond strengths, appropriate for the target of the above study.

Acknowledgment

M.F.B. thanks the Greek Ministry of National Economy for a fellowship (2000).

References

[1] IUPAC special issue: the first century of physical organic chemistry, Pure Appl. Chem. 69 (1997) 211.
[2] X.-K. Jiang, Acc. Chem. Res. 30 (1997) 283.
[3] J.A. Pincock, Acc. Chem. Res. 30 (1997) 43.
[4] H.E. Zimmerman, J. Phys. Chem. A102 (1998) 5616.
[5] N.S. Allen, Photopolymerization and Photoimaging Science and Technology, Elsevier, London, 1989.
[6] A.B. Scranton, C.N. Bowman, R. Peiffer (Eds.), Photopolymerization: Fundamentals and Applications, ACS Symposium Series, vol. 673, American Chemical Society, New York, 1997.
[7] D. Oussi, A. Mokrini, E. Chamarro, S. Esplugas, Environ. Technol. 19 (1998) 955.
[8] C. Guillard, J. Disdier, J.M. Herrmann, C. Lehaut, T. Chopin, S. Malato, J. Blanco, Catal. Today 54 (1999) 217.
[9] K.T. Ranjit, I. Willner, S. Bossmann, A. Braun, Res. Chem. Interm. 25 (1999) 733.
[10] N.S. Allen, Polym. Degrad. Stab. 44 (1994) 357.
[11] A. Dubois, M. Canva, A. Brun, F. Chaput, J.P. Boilot, Appl. Optics 35 (1996) 3193.
[12] H. Kaczmarek, A. Kaminska, M. Swiatek, S. Sanyal, Eur. Polym. J. 36 (2000) 1167.
[13] A.M. Sarker, Y. Kaneko, A.V. Nikolaitchik, D.C. Neckers, J. Phys. Chem. A 102 (1999) 5375 and references cited therein.
[14] M.G. Siskos, A.K. Zarkadis, S. Steenken, N. Karakostas, S.K. Garas, J. Org. Chem. 63 (1998) 3251 and references cited therein.
[15] J. Michl, V. Bonacic-Koutecky, Electronic Aspects of Organic Photochemistry, Wiley/Interscience, London, 1990, p. 138, 292, and 374.
[16] M. Klessinger, J. Michl, Excited States and Photochemistry of Organic Molecules, Verlag Chemie, Weinheim, 1995, p. 348.
[17] E. Kassab, J.T. Gleghorn, E.M. Evleth, J. Am. Chem. Soc. 105 (1983) 1746.
[18] K.M. Dunn, K. Morokuma, J. Phys. Chem. 100 (1996) 123.
[19] M.G. Siskos, A.K. Zarkadis, S. Steenken, N. Karakostas, J. Org. Chem. 64 (1999) 1925.
[20] D.A. Tasis, M.G. Siskos, A.K. Zarkadis, S. Steenken, G. Pistolis, J. Org. Chem. 65 (2000) 4274.
[21] J.J.P. Stewart, J. Comp. Chem. 10 (1989) 221.
[22] M.J. Frisch, G.W. Trucks, H.B. Schlegel, P.M.W. Gill, B.G. Johnson, M.A. Robb, J.R. Cheeseman, T.Keith, G.A. Petersson, J. A.Montgomery, K. Raghavachari, M.A. Al-Laham, V.G. Zakrzewski, J.V. Ortiz, J.B. Foresman, J. Cioslowski, B.B.-Stefanov, A. Nanayakkara, M. Challacombe, C.Y. Peng, P.Y. Ayala, W. Chen, M.W. Wong, J.L. Andres, E.S. Replogle, R. Gomperts, R.L. Martin, D.J. Fox, J.S. Binkley, D.J. Defrees, J. Baker, J.P. Stewart, M. Head-Gordon, C. Gonzalez, J.A. Pople, GAUSSIAN94, Revision D.1., Gaussian Inc., Pittsburgh, PA, 1995.
[23] G.P. Ford, P.S. Herman, J. Chem. Soc., Perkin Trans. 2 (1991) 607.
[24] D.B. Adams, J. Chem. Soc., Perkin Trans. 2 (1987) 247.
[25] M.A. Palafox, F.J. Melendez, J. Mol. Struct. (Theochem) 493 (1999) 171.
[26] C.W. Holzapfel, G.J. Kruger, M.S. Van Dyk, Acta Cryst. C43 (1987) 256.
[27] W.B. Tzeng, K. Narayanan, K.C. Shieh, C.C. Tung, J. Mol. Struct. (Theochem) 428 (1998) 231.
[28] W.E. Sinclair, D.W. Pratt, J. Chem. Phys. 105 (1996) 7942.
[29] W.B. Tzeng, K. Narayanan, J. Mol. Struct. 446 (1998) 93.
[30] B. Kim, C.P. Schick, P.M. Weber, J. Chem. Phys. 103 (1995) 6903.
[31] R. Scheps, D. Florida, S.A. Rice, J. Chem. Phys. 61 (1974) 1730.
[32] H.M. Van Noort, P.J. Vergragt, J. Herbich, J.H. Van der Waals, Chem. Phys. Lett. 71 (1980) 5.
[33] S.K. Sarkar, G.S. Kastha, Spectrochim. Acta 48A (1992) 1611.
[34] P.J. Vergragt, J.A. Kooter, J.H. Van der Waals, Mol. Phys. 33 (1977) 1523.
[35] J.P. Guthrie, J. Barker, P.A. Cullimore, J. Lu, D.C. Pike, Can. J. Chem. 71 (1993) 2111.
[36] D.F. McMillen, D.M. Golden, Ann. Rev. Phys. Chem. 33 (1982) 493.

[37] M.W. Chase Jr., NIST-JANAF Themochemical Tables, Fourth Edition, J. Phys. Chem. Ref. Data, Monograph 9 (1998) 1.
[38] W. Tsang, Heats of formation of organic free radicals by kinetic methods, in: J.A. Martinho Simoes, A. Greenberg, J.F. Liebman (Eds.), Energetics of Organic Free Radicals, Blackie Academic and Professional, London, 1996, p. 22.
[39] H.-D. Beckhaus, B. Dogan, J. Schuetzer, S. Hellman, C. Rüchardt, Chem. Ber. 123 (1990) 137.
[40] A.J. Colussi, S.W. Benson, Int. J. Chem. Kinetics 10 (1978) 1139.
[41] B.S. Jursic, J. Mol. Struct. (Theochem) 366 (1996) 103.
[42] T. Brink, M. Haeberlin, M. Jonsson, J. Am. Chem. Soc. 119 (1997) 4239.
[43] R. Breslow, J.L. Grant, J. Am. Chem. Soc. 99 (1977) 7745.
[44] K.B. Clark, D.D.M. Wayner, J. Am. Chem. Soc. 113 (1991) 9363.
[45] P. Politzer, D. Habibollahzadeh, J. Chem. Phys. 98 (1993) 7659.
[46] J.A. Barltrop, J.D. Coyle, Excited States in Organic Chemistry, Wiley, London, 1975, p. 130.
[47] G.C.G. Waschewsky, D.C. Kitchen, P.W. Browning, L.J. Butler, J. Phys. Chem. 99 (1995) 2635.
[48] K.J. Laidler, Chemical Kinetics, Harper Collins Publishers, New York, 1987, p. 71.
[49] R.C. Pearson, J. Am. Chem. Soc. 110 (1988) 2092.
[50] S. Grimme, Chem. Phys. 163 (1992) 313.